

Effects of phosphate and Cr^{3+} on the sorption and transport of Th(IV) on a silica column

Zhang Hongxia, Yuan Jieqiong, Tao Zuyi*

Radiochemistry Laboratory, College of Chemistry and Chemical Engineering, Lanzhou University, Lanzhou, 730000, P.R. China

(Received September 19, 2006)

Six column experiments were performed, and six breakthrough curves (BTCs) and six displacement (desorption) curves (DPCs) were obtained, which demonstrate the effects of phosphate and Cr^{3+} on the sorption and transport of Th(IV) on a silica column at pH 3.0 and Th(IV) concentration $8 \cdot 10^{-6}$ mol/l of the influent. It was found that in the presence of phosphate sorbed preliminarily on the silica column, the amount of Th(IV) sorbed on the silica column is significantly increased. The breakthrough is significantly delayed relative to those in the absence of phosphate; the effect of simultaneous injection of Cr^{3+} on Th(IV) breakthrough is not significant and while the maximum concentration of Th(IV) of BTC is significantly decreased and reached about 70% of the input concentration; a minor proportion of Th(IV) sorbed on the silica column in the presence or absence of phosphate is not readily displaced with 0.01 mol/l KNO_3 aqueous solution at pH 3. Transport and sorption studies of Th(IV) are important, since all thorium isotopes are radioactive, and Th(IV) is an analogue of tetravalent actinides. There is a need to understand the potential for migration from radioactive waste storage and mill tilling sites.

Introduction

In the previous papers from our laboratory,^{1–5} the sorption of Th(IV) on SiO_2 , Al_2O_3 and TiO_2 and the sorption of U(VI) on SiO_2 and Al_2O_3 were studied by the batch technique as a function of pH and ionic strength. We focused on the effect of phosphate on the sorption of Th(IV) and U(VI), and a significantly positive effect of phosphate was found that can be attributed to the strong surface binding of phosphate and the subsequent formation of ternary surface complexes involving metal and phosphate. In general, column experiments^{6,7} can better simulate field conditions than batch experiments, because (1) the transport behavior of heavy metals in porous media, such as aquifers and soils, is controlled by interplay between physical transfer and sorption or/and precipitation reactions of metals, (2) a higher solid/solution ratio is possible, and (3) reaction products do not accumulate. On the other hand, column experiments are often run at high flow velocity, and this leads to underestimation of slow reactions of importance in field low-flow conditions. Therefore, batch and column experiments are complementary for the understanding of the physical-chemical phenomena involved in transport of heavy metals in porous media. This paper is an extension of our previous papers.^{1–7} The first objective of this paper was to investigate the effect of phosphate on the sorption and transport of Th(IV) on a silica column, since phosphate is ubiquitous and silica is abundant in the earth.

In the previous papers,^{1,2} it was found that as a whole, the sorption of Th(IV) is slightly decreased with increasing ionic strength from 0.01 to 0.5 mol/l KNO_3 . However, multivalent metals, such as Cd^{2+} and Cr^{3+} are

very common in the environment as contaminants. Clearly, the competition between Th(IV) and other multivalent metals for sorption sites of surface is of great importance in the study of the sorption and transport behavior of Th(IV). The second objective of this paper was to investigate the effect of trivalent Cr^{3+} on the sorption and transport of Th(IV) on a silica column.

The sorption of Th(IV) on silica was studied by OSTHOLS et al.^{8,9} Batch experiments were carried out and the $^{232}\text{Th}(\text{NO}_3)_4$ as chemical reagent at relatively high total concentrations (10^{-2} – 10^{-6} mol/l) was used. The pH sorption edges were determined and found to be located at $\text{pH} < 4.5$.

Experimental

Commercial silica (spectral pure) was purchased from the Shanghai Wu-Xi Chemical Factory. The conditioning and storage of silica were identical to those already employed.^{1–6} The specific surface area of this silica was $9.8 \text{ m}^2/\text{g}$, the particle size range of 40–120 mesh.

The stock solutions of $\text{Th}(\text{NO}_3)_4$, phosphate and Cr^{3+} were prepared by dissolving $\text{Th}(\text{NO}_3)_4 \cdot 5\text{H}_2\text{O}$, KH_2PO_4 and $\text{CrCl}_3 \cdot 6\text{H}_2\text{O}$ in distilled deionized water. The total concentration of Th(IV) or phosphate was determined by spectrophotometric analysis with Arsenazo-III or phosphomolybdate blue using ascorbic acid as a reducing agent.^{3,4} The exact concentrations of the stock solutions of Th(IV) and phosphate were respectively determined gravimetrically and by weighing.^{1–5} The pH value of input solution was adjusted by adding a small amount of HNO_3 . All chemicals used here were analytical reagent.

* E-mail: taozuyi@lzu.edu.cn

The essential procedures and the instruments of column experiments were identical to those already employed.^{6,7} The column was slurry packed with 1.0 g of conditioned silica. The pore volume (V_0) was measured by the weight difference of the column before and after saturation with water. The column experiment was divided into three parts: (1) before column experiment, the column was percolated and conditioned preliminarily until the pH and the concentration of solute of effluents were equal to those of influent; (2) after pre-conditioning of the column, a pulse of solution was injected to the column at a constant flux, until the maximum concentration of $\text{Th}(\text{IV})$ in effluents was reached; (3) a displacement solution (desorption solution) was introduced to displace $\text{Th}(\text{IV})$ sorbed from the column at the constant flux until the concentration of $\text{Th}(\text{IV})$ in effluents was approached to zero. The concentrations of $\text{Th}(\text{IV})$ and the pH values in effluents were determined and the concentration was expressed as a relative concentration C/C_0 , where C and C_0 are the concentration in the effluent and in the influent, respectively. Six BTCs and six DPCs were obtained as a C/C_0 vs. V/V_0 plot, where V/V_0 is the total number of pore volume injected and displaced through the column, V is the total volume of effluent. The interruption of flow during changing of the mobile phase lasted no more than a few seconds. The mobile phases passed through the column sequentially in six column experiments as follows:

Experiment 1: Pre-conditioning solution – 0.01 mol/l KNO_3 solution at pH 3.0 (also used in experiments 2, 4, 5 and 6), pulse solution – 0.01 mol/l KNO_3 solution containing $1.00 \cdot 10^{-5}$ mol/l $\text{Th}(\text{NO}_3)_4$ at pH 2.97, displacement solution – 0.01 mol/l KNO_3 at pH 3.0 (also used in Experiments 2–6).

Experiment 2: Pulse solution – 0.01 mol/l KNO_3 solution containing $0.87 \cdot 10^{-5}$ mol/l phosphate at pH 3.05.

Experiment 3: Pre-conditioning solution – 0.01 mol/l KNO_3 solution containing $1.09 \cdot 10^{-5}$ mol/l phosphate at pH 3.0, pulse solution – 0.01 mol/l KNO_3 solution containing $0.824 \cdot 10^{-5}$ mol/l $\text{Th}(\text{NO}_3)_4$ at pH 3.04. The pulse solution was injected at $V/V_0 = 61$.

Experiment 4: Pulse solution – 0.01 mol/l KNO_3 solution containing $0.811 \cdot 10^{-5}$ mol/l $\text{Th}(\text{NO}_3)_4$ and $1.0 \cdot 10^{-5}$ mol/l CrCl_3 at pH 3.02.

Experiments 5 and 6: Pulse solutions – 0.01 mol/l KNO_3 solutions containing $0.811 \cdot 10^{-5}$ mol/l $\text{Th}(\text{NO}_3)_4$ and $0.850 \cdot 10^{-5}$ mol/l $\text{Th}(\text{NO}_3)_4$ at pH 2.98.

Results

Experiment 1: The BTC and the DPC of $\text{Th}(\text{IV})$, and the pH value of effluents are shown in Fig. 1. Figure 1 shows the appearance of $\text{Th}(\text{IV})$ after 14 numbers of pore volume and the roughly constant pH 3.0 of

effluents, which was equal to the pH value of influent. As shown in Fig. 1, the C/C_0 was slowly increased before $V/V_0 < 13$ and then abruptly increased from $V/V_0 = 13$ to 23, while in the range of V/V_0 from 23 to 70, the maximum C/C_0 ranged from 0.91 to 0.97. Figure 1 also shows that the DPC was sharply declined and C/C_0 was approached zero at $V/V_0 > 120$.

Experiment 2: The BTC and the DPC of phosphate, and the pH value of effluents are shown in Fig. 2. Figure 2 shows the appearance of phosphate after 4 numbers of pore volume and the sharp increase in C/C_0 before $V/V_0 < 20$. In the range V/V_0 from 20 to 69, the maximum C/C_0 ranged from 0.93 to 1.02. Figure 2 also shows a sharp fall and a little tailing over 21 numbers of pore volume in the DPC after $V/V_0 = 70$.

Experiment 3: The BTC and the DPC of phosphate, the BTC and the DPC of $\text{Th}(\text{IV})$, and the pH value of effluents are shown in Fig. 3. As shown in Fig. 3, the C/C_0 of phosphate was abruptly increased before $V/V_0 < 15$ and then reached the maximum concentration $C/C_0 > 1$ over 30 numbers of pore volume, later on the C/C_0 was abruptly decreased with a little tailing. In contrast to Fig. 1 in the absence of phosphate sorbed on the silica column, the BTC in Fig. 3 shows the protracted appearance of $\text{Th}(\text{IV})$ after 17 numbers of pore volume of pulse solution in the presence of phosphate. As shown in Fig. 3, the C/C_0 was abruptly increased over 10 numbers of pore volume and then reached a steady maximum concentration C/C_0 ranging from 0.97 to 1.01 over 90 numbers of pore volume. The DPC in Fig. 3 also shows that the $\text{Th}(\text{IV})$ was sharply declined and approached to zero at 250 pore volume with a little tailing.

Experiment 4: The BTC and the DPC of $\text{Th}(\text{IV})$ in the presence of Cr^{3+} in the pulse solution are shown in Fig. 4. Like the BTC in the absence of Cr^{3+} in the pulse solution (Fig. 1), Fig. 4 also shows the appearance of $\text{Th}(\text{IV})$ shortly after 10 pore volume and the slow increase in C/C_0 before $V/V_0 < 16$ and fast increase in C/C_0 from V/V_0 16 to 36. As shown in Fig. 4, in contrast to Fig. 1 in the absence of Cr^{3+} in the pulse solution, the maximum concentration C/C_0 ranged from 0.74 to 0.64 in the range of V/V_0 36–76. The DPC of $\text{Th}(\text{IV})$ was sharply declined over 40 numbers of pore volume with a little tailing after $V/V_0 = 120$.

Experiment 5: Figure 5 shows the effect of flow rate on the BTC and the DPC of $\text{Th}(\text{IV})$ on the silica column. At slower flow rate the BTC was shifted to the right as compared with that at higher flow rate (Fig. 1). The maximum concentration at slower flow rate was slightly lower than that at higher flow rate.

Experiment 6: The BTC and the DPC of $\text{Th}(\text{IV})$ on a silica column with a height of 91 mm are shown in Fig. 6. Figures 6 and 1 show that both the BTCs with different column heights merged into a single one and

both the DPCs at different flow rates were roughly parallel before pore volume 100.

All column parameters are listed in Table 1.

Discussion

As mentioned in the Experimental section, column experiments in this study were designed with a pH 3.0 and a relatively high concentration of Th(IV) to be as simple as possible in order to yield unambiguous results over a limited timescale. Firstly, as shown in Fig. 4 of the previous paper,³ the sorption % of Th(IV) onto silica at pH 3 is about 15% and relatively low as compared

with sorption 80% at pH 4, and the sorption edge of Th(IV) onto silica is practically independent of the ionic strength from 0.001 to 0.1 mol/l. Secondly, at pH 3.0, the free Th⁴⁺ is the predominating species of Th(IV), the hydrolysis of Th(IV) is not significant, furthermore the complexation of Th(IV) with carbonate from air can be negligible. As shown in all Figs 1–6, the pH value of effluents in all column experiments is roughly constant at pH 3 after pre-conditioning. Thus we can definitely rule out the effect of pH on BTC and DPC, and the effects of phosphate and Cr³⁺ on the sorption and transport of Th(IV) on a silica column can be definitely revealed, since both the effects may be concealed from the variation of pH values of effluents.

Table 1. Experimental conditions and results

Column experiment	1	2	3	4	5	6
Column height, mm	76	73	71	72	74	91
Inner diameter, <i>r</i> , mm	7	7	7	7	7	7
Mass of SiO ₂ , g	1.0	1.0	1.0	1.0	1.0	1.2
Pore volume <i>V</i> ₀ , ml	1.27	1.23	1.17	1.20	1.24	1.52
Flow rate, ml/min	0.50	0.50	0.65	0.61	0.33	0.61
¹ Pulse length, <i>V/V</i> ₀	79	73	133	81	59	72
² Displacement length, <i>V/V</i> ₀	88	32	89	112	79	112
³ <i>Q</i> ₀ , ×10 ⁻⁷ mol/g	1.92	1.18	2.60	1.62	2.08	2.01
⁴ <i>Q</i> , ×10 ⁻⁷ mol/g	1.40	0.58	1.38	1.02	1.25	1.58
Recovery rate, %	73	49	53	63	60	78
⁵ <i>E</i> , min	27	25	26	20	39	28

¹ Pulse length: Duration of injection of pulse solution to the column.

² Displacement length: Duration of injection of displacement solution to the column.

³ *Q*₀: Amount of Th(IV) sorbed on 1 g silica.

⁴ *Q*: Amount of Th(IV) desorbed from 1 g silica.

⁵ *E*: Mean residence time.

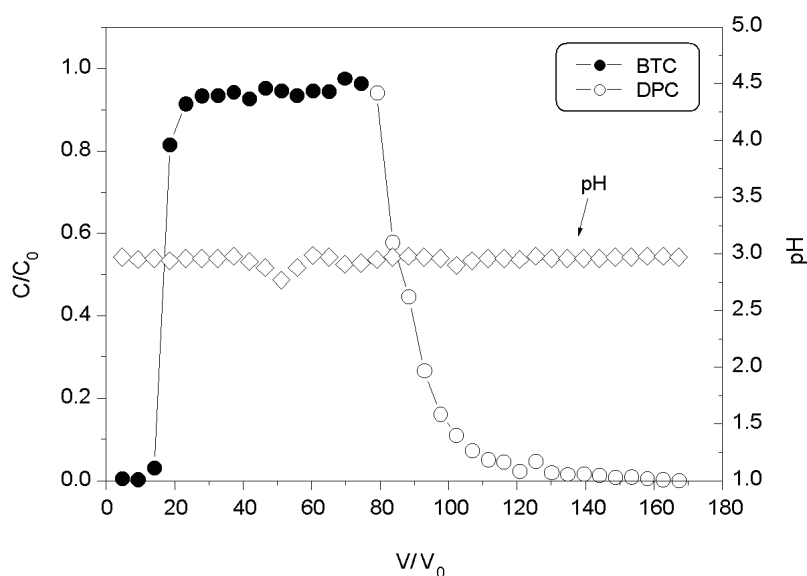


Fig. 1. The BTC (●) and the DPC (○) of Th(IV) on a silica column, and the pH value of effluents

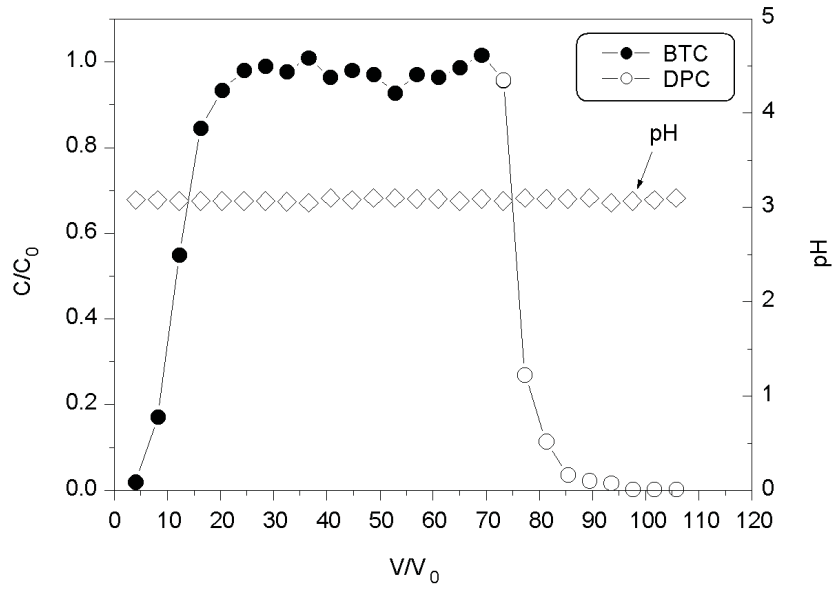


Fig. 2. The BTC (●) and the DPC (○) of phosphate on a silica column, and the pH value of effluents

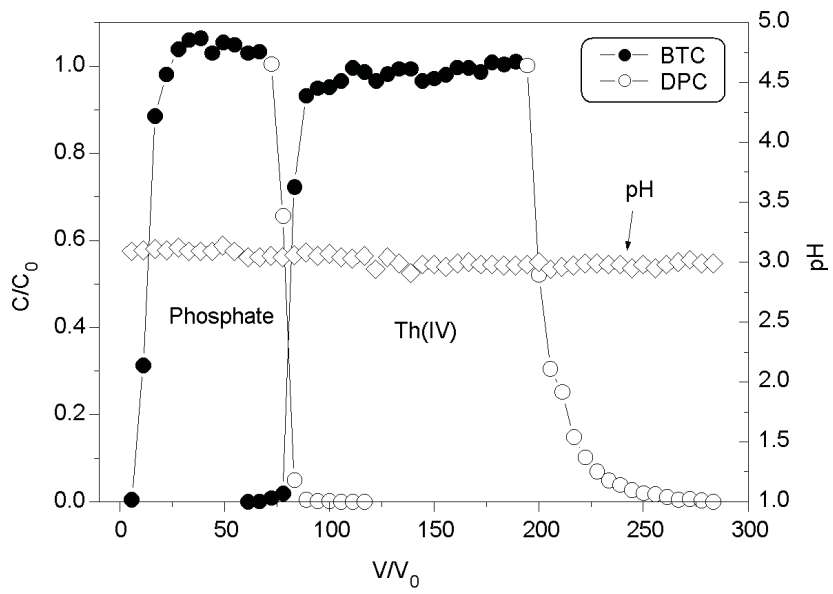


Fig. 3. The BTC (●) and DPC (○) of phosphate, the BTC (●) and the DPC (○) of Th(IV) on a silica column, and the variation of pH values of effluents

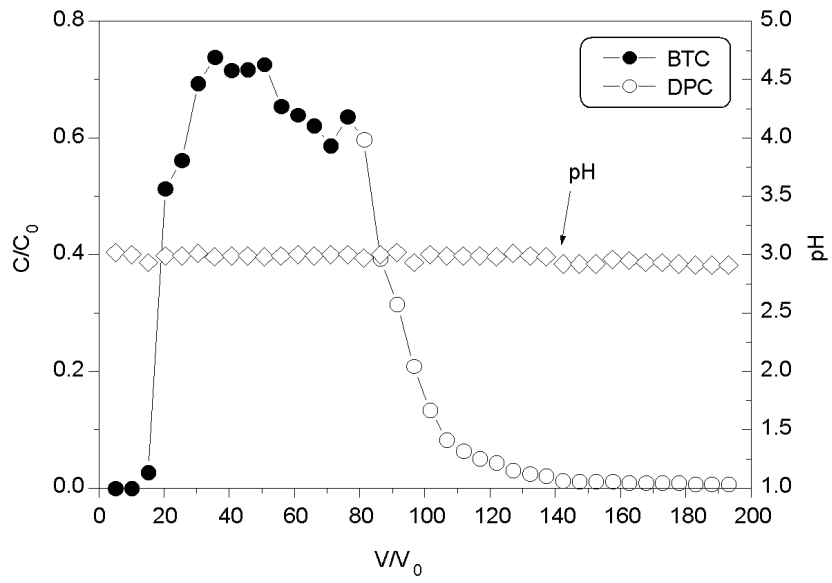


Fig. 4. The BTC (●) and the DPC (○) of Th(IV) on a silica column in the presence of co-injection of Cr^{3+} , and the pH value of effluents

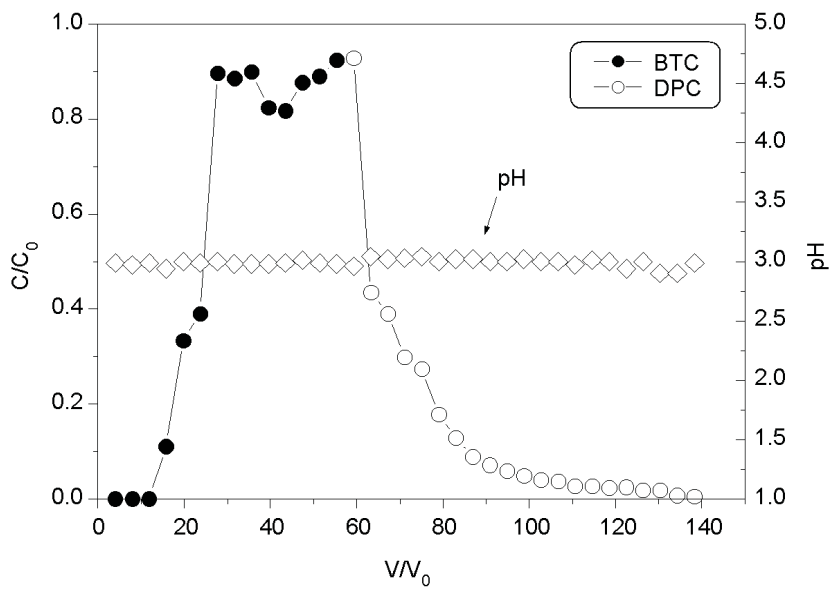


Fig. 5. The BTC (●) and DPC (○) of Th(IV) on a silica column at slower flow rate ($u = 0.33$ ml/min), and the pH value of effluents

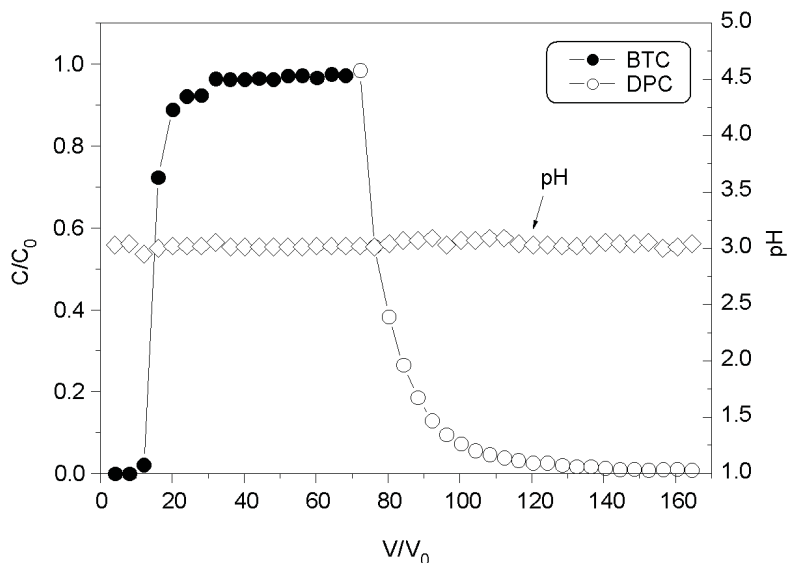


Fig. 6. The BTC (●) and the DPC (○) of Th(IV) on the silica column with a height of 91 mm, and the pH value of effluents

The moment analysis can be used to interpret the BTC. The n -th moment is defined by:^{10,11}

$$M(t^N) = \int_0^{\infty} t^N \frac{C(t)}{C_0} dt \quad (1)$$

where C_0 is the concentration of influent imposed for $0 < t < T_0$ (pulse length). The zero order moment is used for the mass balance and the first order moment is used in the calculation of the mean residence time, E . Expression for E is given by:

$$E = \frac{M(t^1)}{M(t^0)} \quad (2)$$

The amount of Th(IV) sorbed on 1 g silica (Q_0) and the amount of Th(IV) desorbed from 1 g silica (Q) were, respectively, calculated from the difference between the zero order moment of BTC and the amount of Th(IV) in the pulse solution from $t=0$ to $t=T_0$ and the area beneath DPC. The $M(t^0)$ and the area beneath DPC were obtained by the trapezoid rule integration. The values of Q_0 and Q of all column experiments are listed in Table 1 too.

Table 1 shows that the value of Q_{03} in the presence of phosphate sorbed preliminarily is 1.4 times as large as Q_{01} in the absence of phosphate; and that value of Q_{05} at slower flow rate is increased about 8% as compared with that at higher flow rate. Both the increases in Q_0 indicate that besides the surface hydroxyl groups on silica, the phosphate ions sorbed preliminarily on the surface of silica also act as sorption sites with high affinity for Th(IV), and that at both flow rates used in this paper, the sorption process in the dynamic system studied here is far from equilibrium. As shown in Table 1, recovery

rates range from 53% in the presence of phosphate sorbed to 73% in the absence of phosphate. These recovery rates indicate that a minor proportion of Th(IV) bound to the surface hydroxyl groups is not readily recoverable, and that a minor proportion of Th(IV) bound to phosphate sorbed on silica are also not readily recoverable. A comparison of Figs 1 and 5 indicate that the recovery rate is increased with increasing flow rate, suggesting that the higher flow rate decreases the thickness of liquid film on surface and increases the desorption rate.

Figure 3 shows that almost 17 numbers of pore volume are needed to be injected before breakthrough in the presence of phosphate sorbed. While Fig. 1 shows that only 14 numbers of pore volume are needed to be injected before breakthrough in the absence of phosphate. As shown in Table 1 and Fig. 3, in spite of lower column and higher flow rate as compared with Experiment 1, the mean residence time of Th(IV) in the presence of phosphate is equal to that in the absence of phosphate. All these results demonstrate that the phosphate sorbed on the silica column actively retards the migration of Th(IV).

A comparison of Figs 1 and 4 indicates that in the presence and absence of Cr^{3+} in the pulse solution, almost the same numbers of pore volume are needed to be injected before breakthrough. As shown in Table 1, the mean residence times in the presence and absence of Cr^{3+} are not significantly different each other. Thus it may be concluded that the effect of Cr^{3+} on the migration of Th(IV) on the silica column is not significant, though the maximum concentration of Th(IV) in the presence of Cr^{3+} is decreased by 30%.

Conclusions

From the experimental results and discussion, it may be concluded as follows: (1) Phosphate exerts a significant control on the Th(IV) sorption and transport on the silica column. (2) The breakthrough of Th(IV) on the silica column is not significantly influenced by the co-injection of Cr³⁺. (3) A minor proportion of Th(IV) sorbed on the silica column in the presence and absence of phosphate sorbed preliminarily is not readily desorbed and recoverable. This work suggests that the effects of competing cations and inorganic ligands on the sorption and transport of tetravalent actinides are very important in the assessment of the long term interactions of tetravalent actinides with the environment in radioactive waste storage and mill tilling sites.

*

This project was supported by the National Natural Science Foundation of China (Grant No. 20501010).

References

1. Z. J. GUO, L. J. NIU, Z. Y. TAO, *J. Radioanal. Nucl. Chem.*, 266 (2005) 333.
2. Z. J. GUO, X. M. YU, F. H. GUO, Z. Y. TAO, *J. Colloid Interface Sci.*, 288 (2005) 14.
3. W. J. LI, Z. Y. TAO, *J. Radioanal. Nucl. Chem.*, 254 (2002) 157.
4. H. X. ZHANG, Z. Y. TAO, *J. Radioanal. Nucl. Chem.*, 254 (2002) 103.
5. Z. J. GUO, F. H. GUO, Z. Y. TAO, *Radiochim. Acta*, 94 (2006) 223.
6. W. J. LI, Z. Y. TAO, L. T. GUO, S. S. LI, *Radiochim. Acta*, 91 (2003) 575.
7. X. K. WANG, W. M. DONG, G. WANG, Z. Y. TAO, *Appl. Radiation Isotopes*, 56 (2000) 765.
8. E. OSTHOLS, A. MANCEAN, F. FARGES, L. CHARLET, *J. Colloid Interface Sci.*, 194 (1997) 10.
9. E. OSTHOLS, *Geochim. Cosmochim. Acta*, 59 (1995) 1235.
10. A. I. KALINICHEV, A. YA. PRONIN, K. V. CHMUTOV, N. A. GORYACHEVA, *J. Chromatography*, 152 (1978) 311.
11. U. GABRIEL, J-P. GAUDET, L. SPADIMI, L. CHARLET, *Chem. Geol.*, 151 (1998) 107.